NACA

RESEARCH MEMORANDUM

PRELIMINARY EXPERIMENTAL INVESTIGATION OF FLUTTER

CHARACTERISTICS OF M AND W WINGS
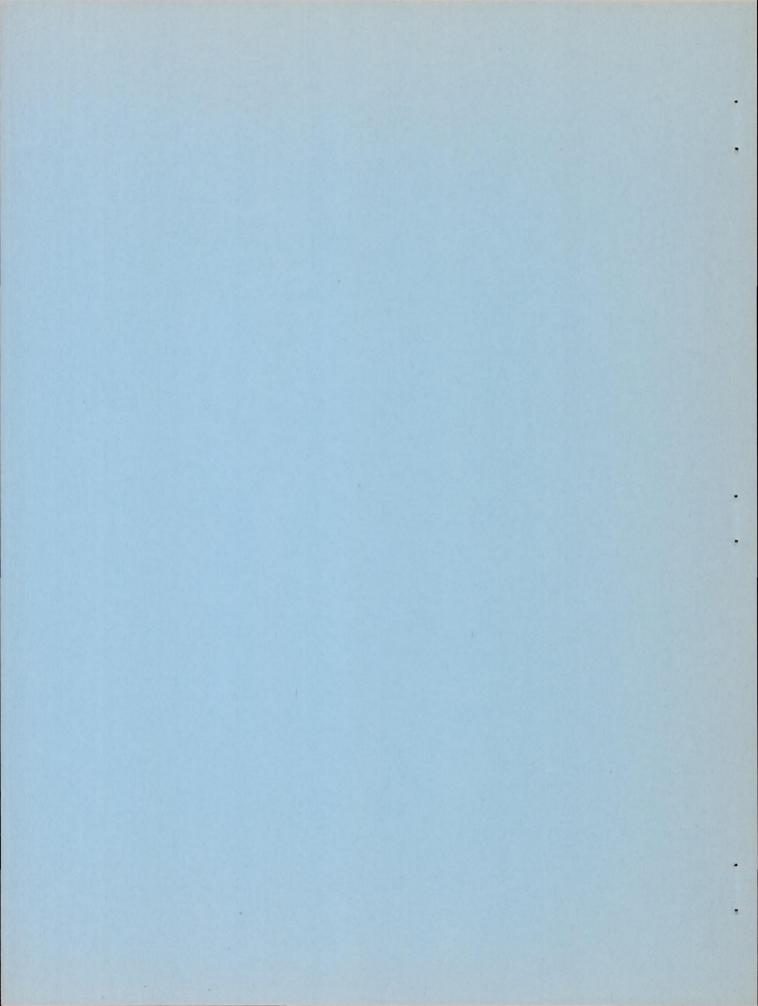
By Robert W. Herr

Langley Aeronautical Laboratory
Langley Field, Va.

NATIONAL ADVISORY COMMITTEE
FOR AERONAUTICS

WASHINGTON

August 8, 1951

NATIONAL ADVISORY COMMITTEE FOR AERONAUTICS

RESEARCH MEMORANDUM

PRELIMINARY EXPERIMENTAL INVESTIGATION OF FLUTTER

CHARACTERISTICS OF M AND W WINGS

By Robert W. Herr

SUMMARY

Results of nine experimental flutter tests involving two flat-plate models and two rib and spar models of NACA 0012 airfoil section are presented to give a comparison of the flutter characteristics of wings having M and W type plan forms. Within the range of structural and aerodynamic parameters encountered in these tests, the W plan form gave higher flutter speeds than the M plan forms.

A technique is also presented in an appendix whereby the natural vibration mode shapes of the model wings were obtained photographically. These mode shapes, along with the other structural parameters included, would be useful in a theoretical flutter analysis of the M and W wing configurations.

INTRODUCTION

Some attention has been given recently to the possibility of the use of wings incorporating sweepback of the inboard panel and sweepforward of the outboard panels (W plan forms) or vice versa (M plan forms) for high speed aircraft. It has been suggested that such configurations might display better stability and deflection characteristics than the swept-back wing without appreciable sacrifice of the low-drag qualities of the latter. Some investigations along these lines have been made in references 1 and 2.

In order to obtain some idea as to the relative flutter characteristics of the M and W configurations, tests were made in the Langley 4.5-foot flutter tunnel of two sets of models having M and W plan forms. One series of tests was made with extremely simplified models consisting of flat plates of 0.128-inch aluminum alloy. Other tests were made with models of rib and spar construction built to NACA 0012 airfoil shape. The results of the flutter experiments are discussed and a technique is

described for obtaining photographically the natural vibration mode
shapes of the model wings.

SYMBOLS

b   semichord of wing in stream direction

f_n natural vibration frequencies in the nth mode, cycles
                per second

I_{CG} polar mass moment of inertia about section center of gravity
                for a strip in the stream direction of one foot width,
                slug-feet

l length of semispan model measured normal to stream direction

m   mass of wing per foot of span measured normal to stream
                direction, slugs per foot

M   Mach number at flutter

v   airspeed at flutter, feet per second

κ mass ratio, $\left(\dfrac{\int_0^l \pi\rho b^2 dx}{m_{total}}\right)$

ρ density of testing medium, slugs per cubic foot

ω angular flutter frequency, radians per second

APPARATUS

Wind tunnel.- The flutter tests were made in the Langley 4.5-foot
flutter tunnel. This tunnel is of the closed throat single-return type
in which the pressure may be varied from approximately 0.5 inch of
mercury absolute to atmospheric pressure.

Models.- The four models employed in these tests were 24-inch semi-
span cantilevers with a taper ratio of approximately 0.5 and a full-span
aspect ratio of 2.66. The midchord line of the inboard half of the
W wings was swept back at an angle of 45° and the outboard half was swept

forward at an angle of 45°. Sweep angles on the M wings were opposite in direction from those of the W wings.

The first model tested (model A) was cut from a 0.128-inch flat plate of 24ST aluminum alloy and was of the same plan form as the model sketched in figure 1. This model was tested as both an M and W configuration by reversing its position in the test section. The subscripts m and w added to the model designation denote the position of the model in the test section. The second model tested, designated B_s, was used as a reference model and was also a 0.128-inch flat plate of the same semispan, taper ratio, and aspect ratio as model A but with the entire semispan swept back at an angle of 45°. The section centers of gravity of the flat-plate models were, of course, at the midchord.

The third and fourth models were constructed to have more realistic structural parameters than the simplified models and incorporated NACA 0012 airfoil sections in the stream direction. One model is of W plan form and is designated C_w; the other of M plan form is designated D_m. The models were of single-spar construction with very closely spaced ribs and were covered with rubber (figs. 1 and 2). The small lead weights which are noticed in figure 2 were inserted between each rib to make the section centers of gravity coincide. The section centers of gravity for both models were at 40 percent chord over the inboard half and at 45 percent chord over the outboard half.

DETERMINATION OF MODEL PARAMETERS

Although the investigation described herein was of an experimental nature, it was considered desirable to obtain some of the structural parameters of the models so that a reader who wishes to make theoretical flutter calculations for the models may do so. These parameters include the vibration mode shapes, the spanwise variation of mass and mass moment of inertia, and the loci of flexural centers.

The unorthodox plan forms of these models indicate that the calculation of the natural vibration mode shapes would be difficult. The mode shapes were, therefore, obtained experimentally by exciting the wings at their natural vibration frequencies and photographing the resulting amplitudes. (See appendix.)

Variations along the span (normal to stream direction) of the mass and the mass moment of inertia are plotted in figures 3 and 4.

The loci of flexural centers of the models (fig. 5) were determined as follows. The wing was clamped rigidly at the root and at a given spanwise station was loaded successively at various chordwise points lying in

the stream direction until the point was found where no twist in the
stream direction occurred at that station. This procedure was repeated
at several spanwise stations until enough points were obtained to permit
a smooth curve to be drawn.

The natural vibration frequencies of the models were obtained with
the aid of a calibrated electronic oscillator driving a magnetic shaker
which in turn excited the wings. The frequencies so obtained are as
follows:

Model	f_1	f_2	f_3	f_4
A	8.0	18.9	49	----
B_s	5.9	24.8	39	57.5
C_w	6.0	13.4	40	63.0
D_m	5.6	16.8	42	----

TEST PROCEDURE

Since flutter is generally a destructive phenomenon it is necessary
to exercise great care during a flutter test. The tunnel speed was,
therefore, increased slowly during the runs, the increases amounting to
smaller increments as the critical flutter speed was approached. At the
critical flutter speed, the necessary tunnel data were recorded and an
oscillograph record of the model deflections were taken. The tunnel
speed was then immediately reduced in order to preserve the model.

In these tests, the tunnel was operated at pressures from 0.25 atmos-
phere to atmospheric pressure, and at Mach numbers up to 0.60. The
Reynolds numbers at flutter varied from 1.2×10^6 to 3.6×10^6.

A total of nine tests was made. These tests included two for the
flat-plate model A (one in the M position and one in the W position),
one for the flat-plate swept wing model B_s, and three each for the W and
M plan forms of NACA 0012 section (C_w and D_m).

In order to ascertain whether the model had been damaged or weakened
by flutter, oscillograph records were taken before and after each run at
zero airspeed with the model manually excited at its first and second
natural frequencies. These frequencies did not change a measurable amount
throughout the series of tests.

RESULTS AND DISCUSSION

Table I lists the experimental flutter velocities, the corresponding values of the mass ratio parameter $\sqrt{1/\kappa}$, the flutter frequency ω, and the associated values of Mach number and air density.

The critical flutter frequencies were obtained from oscillograph records taken at flutter. A sample record taken at flutter (v = 427.6, table I) is shown as figure 6. This model, D_m, fluttered to destruction during this run before the tunnel speed could be reduced.

In figure 7 the flutter velocities are plotted against the mass ratio parameter $\sqrt{1/\kappa}$. The significance of such a plot lies in the fact that a given model will usually flutter at a velocity which is essentially proportional to $\sqrt{1/\kappa}$ provided there is no change in flutter mode (reference 3).

Inspection of figure 7 shows the single value of flutter speed obtained for the flat-plate model A in the W position to be approximately 25 percent higher than for the same model in the M position whereas the flutter speed of the swept flat-plate reference model B_s fell between those obtained for the M and W configurations. The NACA 0012 section W model C_w showed an even greater increase in flutter speed over the corresponding M wing D_m, the difference being about 50 percent throughout the range of mass ratio parameters investigated.

Caution should be used in generalizing the results of this investigation as the flutter speed is dependent on the relationship of numerous structural and aerodynamic parameters, a change in any of which may alter the conclusions. For example, aspect ratio may have an important bearing on the relative flutter and divergence speeds.

CONCLUDING REMARKS

Within the range of structural and aerodynamic parameters encountered in these tests the W wing plan form gave higher values of flutter speed than the M plan form.

Natural vibration mode shapes, obtained photographically, along with other pertinent structural parameters have been included to aid in a theoretical flutter analysis of these wing configurations.

Langley Aeronautical Laboratory
        National Advisory Committee for Aeronautics
                Langley Field, Va.

APPENDIX

EXPERIMENTAL DETERMINATION OF NATURAL VIBRATION MODES

The natural vibration modes were obtained photographically with the aid of two electronic flash lamps having a flash duration of 1/5000 second. The wing was excited at its natural vibration frequencies by a calibrated electronic oscillator driving a magnetic shaker. The amplitude of the oscillations was increased until the wing tip contacted two pairs of very flexible wires, thus completing electrical circuits and firing the flash lamps at the maximum positive and negative amplitudes of the vibration cycle.

The camera was mounted approximately 12 feet outboard and 2 feet above the tip of the wing. The wing was painted black with very thin stripes of white running in the stream direction every tenth of the semi-span to make possible the measurements of deflections.

Sample photographs taken by this method appear in figure 8. The deflection amplitudes measured from these photographs must be corrected for perspective; thus the actual value of the deflection amplitude at station n is given by the equation $y_n = y_n'(c_n/c_n')$ where c_n is the actual chord of the model at station n, c_n' is the chord at station n as measured from the photograph, and y_n' is the amplitude at station n as measured from the photograph.

Because of the large amount of structural coupling inherent in the M and W plan forms, the modes shown in figures 9 to 21 were not plotted in the conventional manner, but as three-dimensional views adapted to give the relative deflection at any point on the wing. Since the torsional displacements involved are small, the torsional component of the natural vibration modes may be obtained from figures 9 to 21 by simply subtracting the leading-edge amplitude from the trailing-edge amplitude and dividing by the actual chord of the model; that is

$$\alpha = \frac{y_{n_{TE}} - y_{n_{LE}}}{c_n}$$

Some idea of the accuracy of this photographic method is indicated in figure 22, which shows the photographically obtained experimental vibration modes as well as the theoretical vibration modes of a rectangular 8- by 50- by 0.25-inch flat aluminum-alloy plate mounted as a cantilever. Changing the point of attachment of the exciter to the wing made no measurable difference in the deflection curves.

REFERENCES

1. Campbell, George S., and Morrison, William D., Jr.: A Small-Scale
   Investigation of "M" and "W" Wings at Transonic Speeds. NACA
   RM L50H25a, 1950.

2. Katz, Ellis, Marley, Edward T., and Pepper, William B.: Flight
   Investigation at Mach Numbers from 0.8 to 1.4 to Determine the Zero-
   Lift Drag of Wings with "M" and "W" Plan Forms. NACA RM L50G31,
   1950.

3. Castile, George E., and Herr, Robert W.: Some Effects of Density and
   Mach Number on the Flutter Speed of Two Uniform Wings. NACA
   TN 1989, 1949.
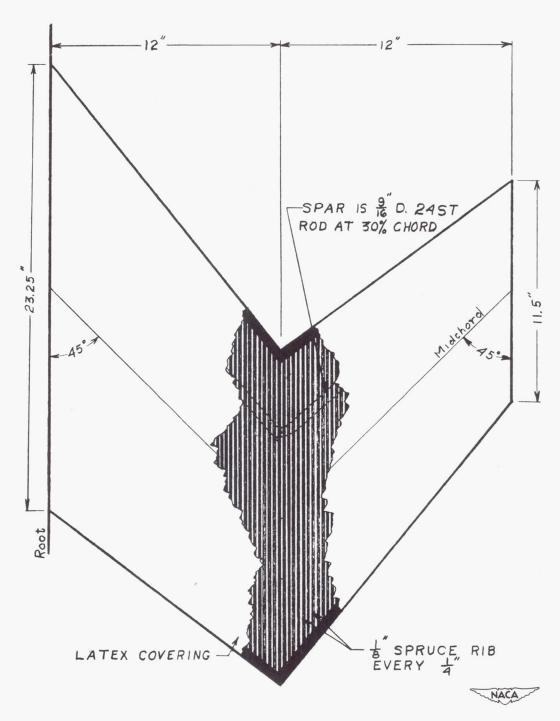
TABLE I

EXPERIMENTAL FLUTTER DATA

Model	ρ (slugs/cu ft)	v (ft/sec)	Mach number, M	ω (radians/sec)	$\sqrt{1/\kappa}$
A_w	0.002294	390.1	0.3522	93.0	4.75
A_m	.002322	312.2	.2820	90.0	4.71
B_s	.002036	354.5	.2990	111.0	5.03
C_w	.002154	376.0	.3300	62.8	5.19
	.001369	461.9	.4095	62.8	6.50
	.000589	669.8	.5970	62.8	9.92
D_m	.002172	250.1	.2169	64.1	5.26
	.001497	299.5	.2595	62.2	6.34
	.000699	427.6	.3715	57.2	9.28

NACA

NACA 0012 AIRFOIL SECTION

Figure 1.- Sketch of model C_w.
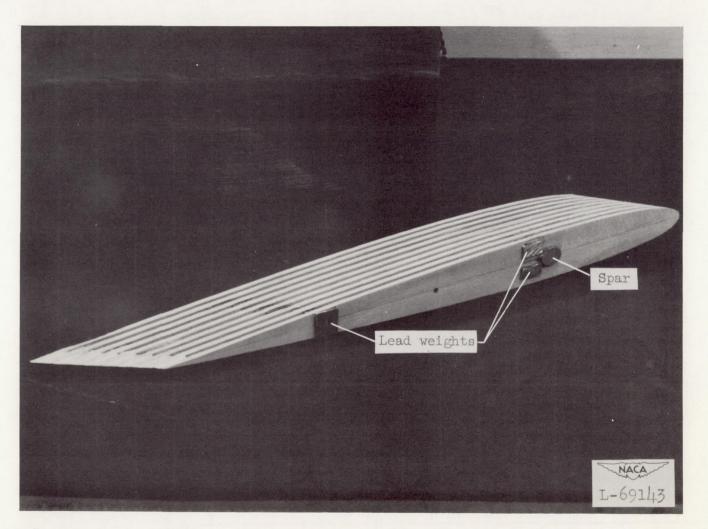
Figure 2.- Photograph of section of model C_w.
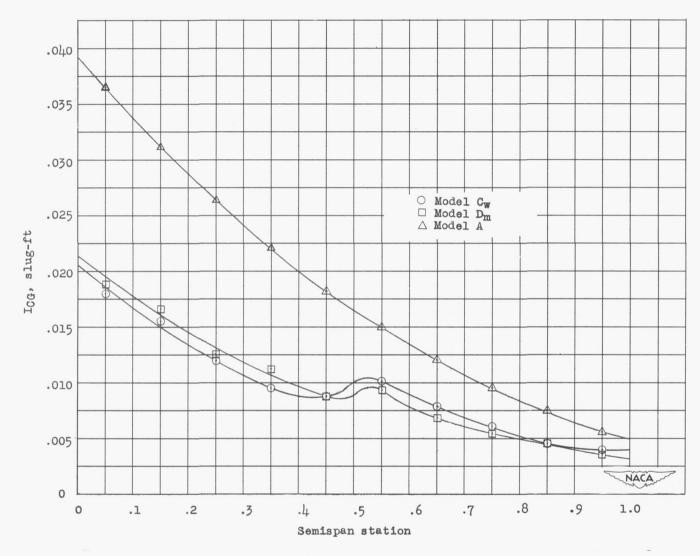
Figure 3.- Variation of mass moment of inertia I_{CG} with span.

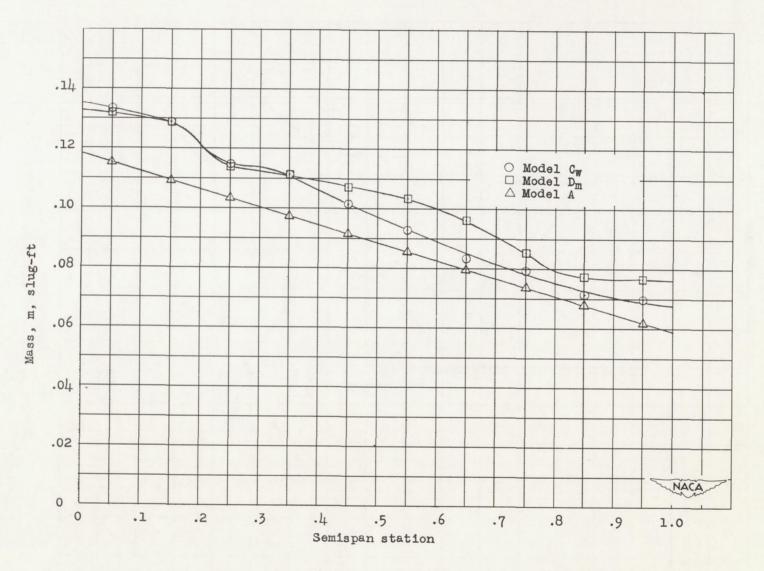Figure 4.- Variation of mass m along semispan.

Figure 5.- Loci of flexural centers.
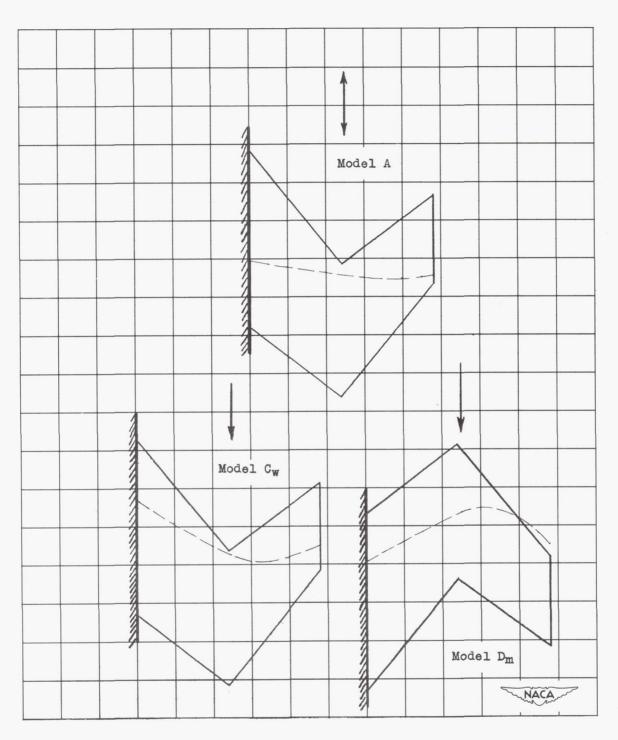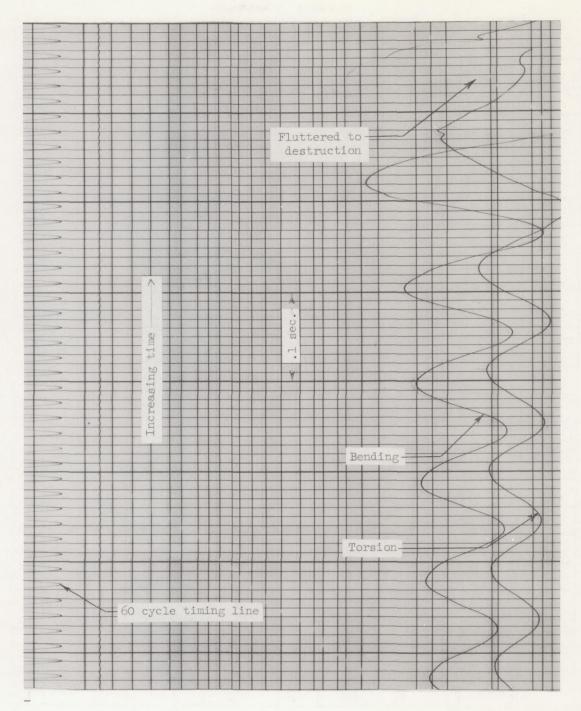
Figure 6.- Sample oscillograph record. Model D_m at flutter.
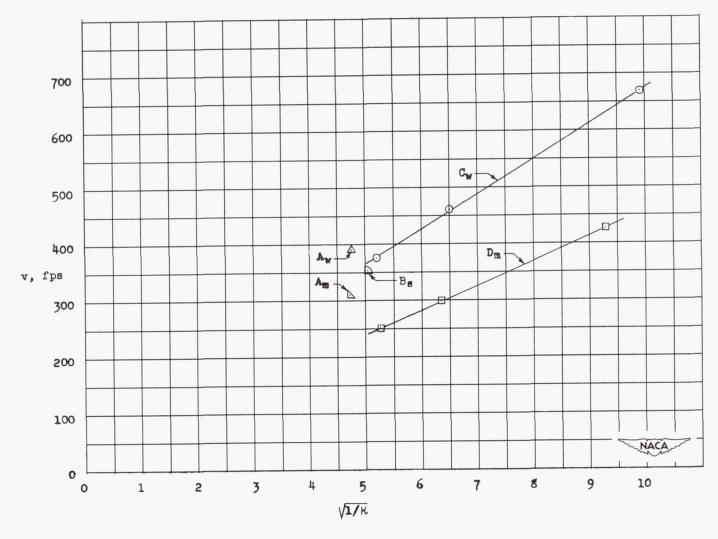
Figure 7.- Variation of the flutter speed v with the mass-ratio
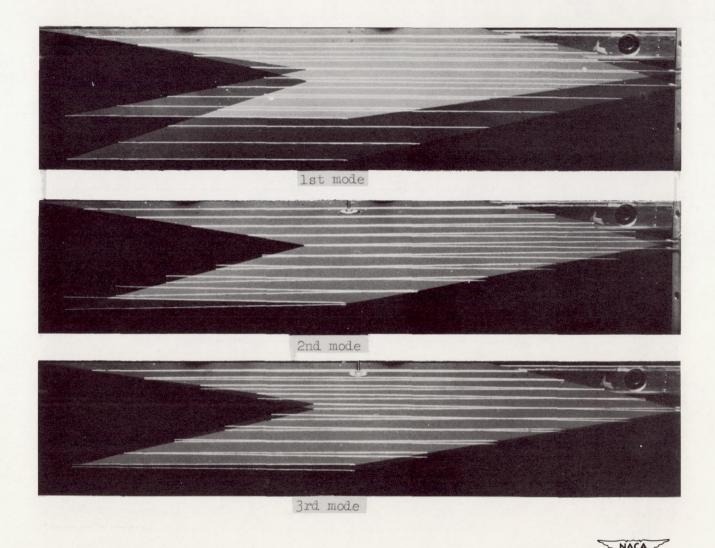parameter $\sqrt{1/\kappa}$.

1st mode

2nd mode

3rd mode

Figure 8.- Photograph of natural vibration modes. Model A. L-69144

Dashed lines indicate shape
of wing at maximum
amplitude of cycle

1.0

.9

.8

.7

.6

Solid lines indicate position
of wing at rest

.5

.4

.3

.2

.1

Fraction of semispan

0

Chord

NACA
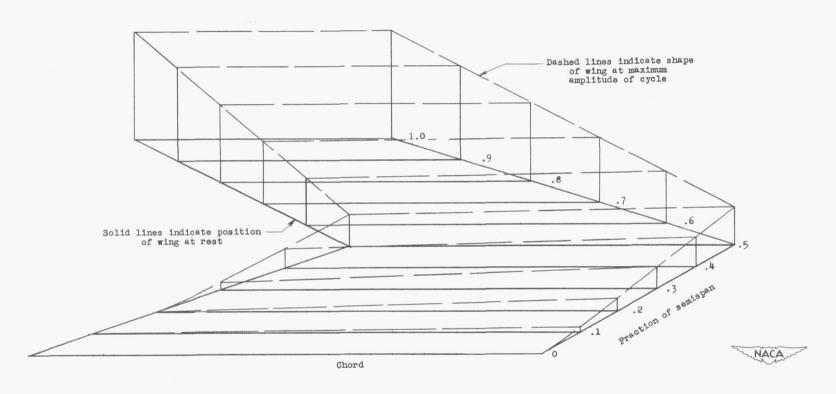
Figure 9.- First natural vibration mode; model C_w.
$f_1 = 6$ cycles per second.

Dots indicate nodal lines

1.0

Dashed lines indicate shape
of wing at maximum
amplitude of cycle

.9

.8

.7

.6

.5

Solid lines indicate position
of wing at rest

.4

.3

Fraction of semispan

.2

.1

Chord

0

NACA
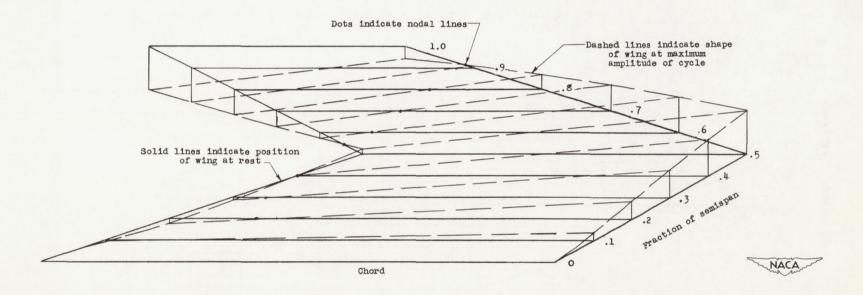
Figure 10.- Second natural vibration mode, model C_w.
$f_2 = 13.4$ cycles per second.

Dots indicate nodal lines

Dashed lines indicate shape
of wing at maximum
amplitude of cycle

1.0

.9

.8

.7

.6

.5

Solid lines indicate position
of wing at rest

.4

.3

.2

Fraction of semispan

.1

0

Chord

NACA
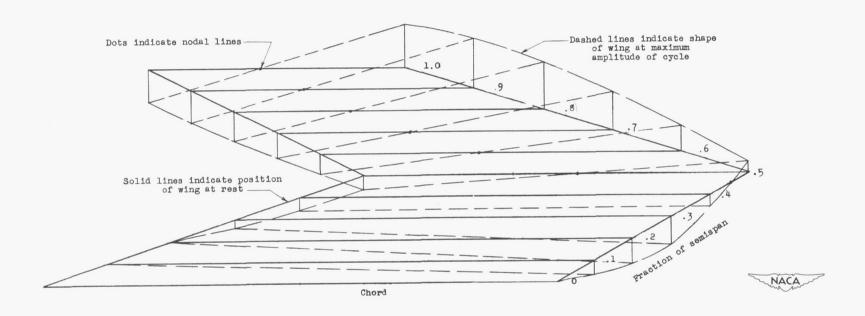
Figure 11.- Third natural vibration mode, model C_W.
$f_3 = 40$ cycles per second.

Dots indicate nodal lines

1.0

.9

Solid lines indicate position
of wing at rest

.8

.7

.6

Dashed lines indicate shape
of wing at maximum
amplitude of cycle

.5

.4

.3

Fraction of semispan

.2

.1

0

Chord

NACA
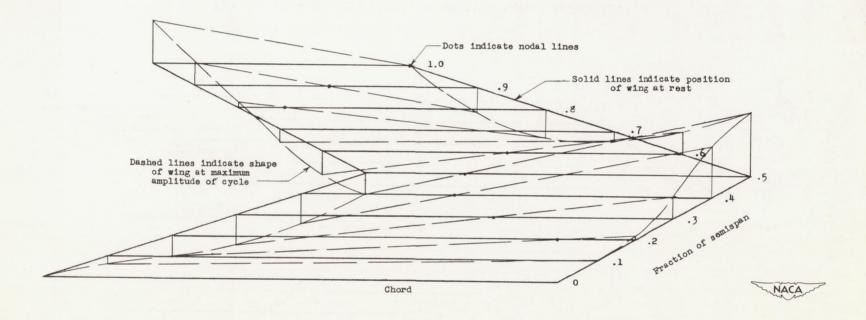
Figure 12.- Fourth natural vibration mode, model C_w.
$f_4 = 63$ cycles per second.

Dashed lines indicate shape
of wing at maximum
amplitude of cycle

Solid lines indicate position
of wing at rest

1.0

.9

.8

.7

.6

.5

.4

.3

.2

.1

0

Fraction of semispan

Chord

NACA

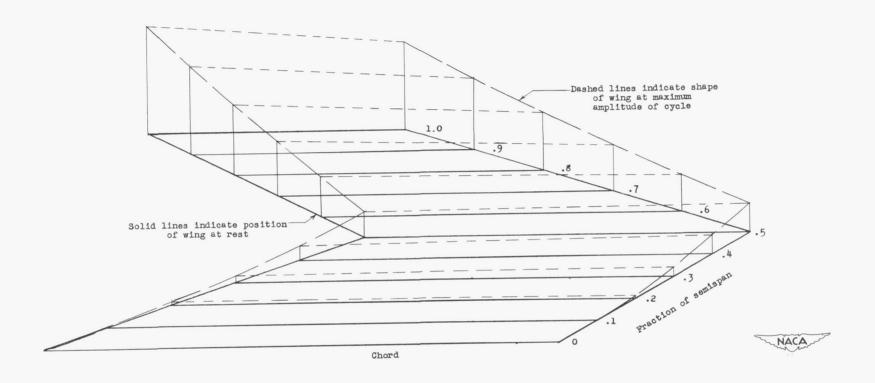Figure 13.- First natural vibration mode, model D_m.
$f_1 = 5.6$ cycles per second.
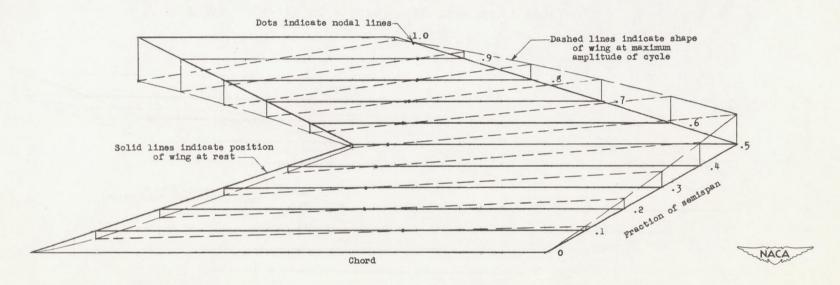
Figure 14.- Second natural vibration mode, model D_m.
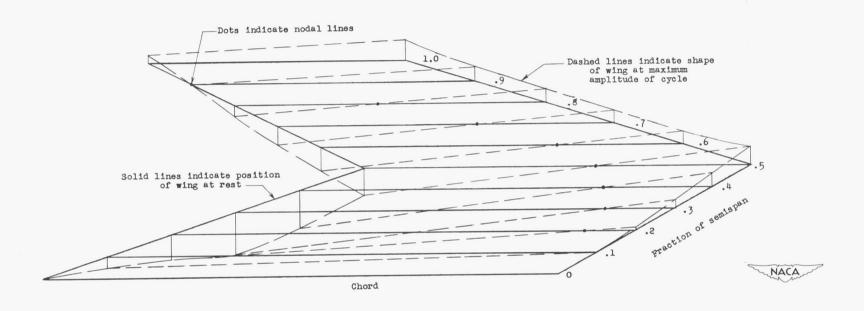f_2 = 16.8 cycles per second.

Dots indicate nodal lines

1.0

.9

.8

Dashed lines indicate shape
of wing at maximum
amplitude of cycle

.7

.6

.5

Solid lines indicate position
of wing at rest

.4

.3

Fraction of semispan

.2

.1

0

Chord

NACA

Figure 15.- Third natural vibration mode, model D_m.
f_3 = 42 cycles per second.

Dashed lines indicate shape
of wing at maximum
amplitude of cycle

1.0

.9

.8

.7

.6

Solid lines indicate position
of wing at rest

.5

.4

.3

.2

Fraction of semispan

.1

0

Chord

NACA

Figure 16.- First natural vibration mode, model A.
$f_1 = 8$ cycles per second.

Dots indicate nodal lines

Dashed lines indicate shape
of wing at maximum
amplitude of cycle

1.0

.9

.8

.7

.6

.5

.4

Solid lines indicate position
of wing at rest
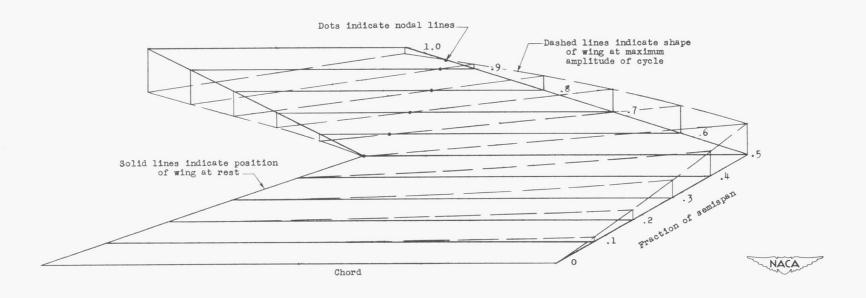
.3

.2

Fraction of semispan

.1

0

Chord

NACA

Figure 17.- Second natural vibration mode, model A.
$f_2 = 18.9$ cycles per second.

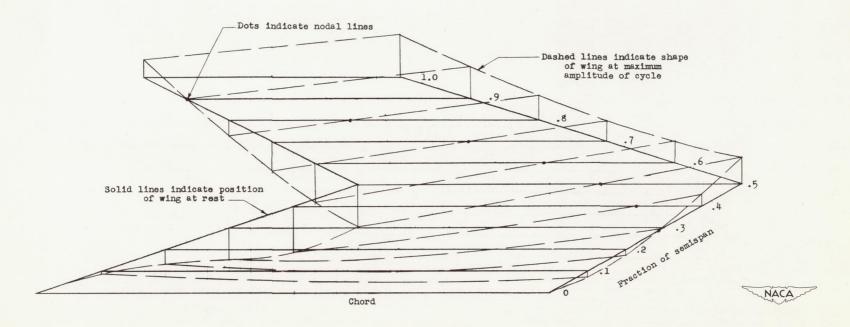Figure 18.- Third natural vibration mode, model A.
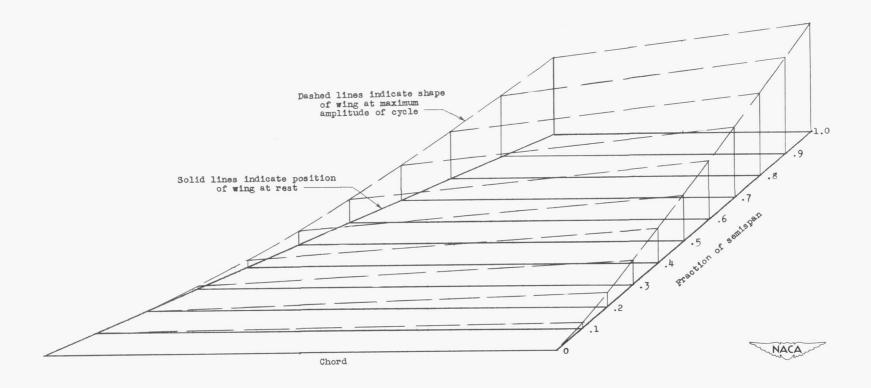f_3 = 49 cycles per second.

Dashed lines indicate shape
of wing at maximum
amplitude of cycle

Solid lines indicate position
of wing at rest

Fraction of semispan

Chord

Figure 19.- First natural vibration mode, model B_s.
$f_1 = 5.9$ cycles per second.

Figure 20.- Second natural vibration mode, model B_s.
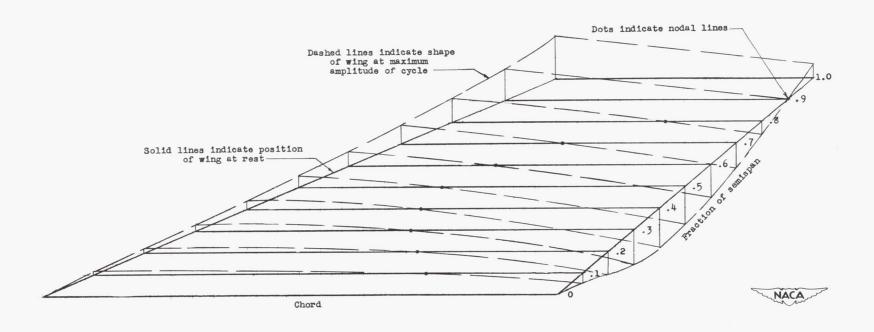
$f_2 = 24.8$ cycles per second.

Dots indicate nodal lines

Dashed lines indicate shape
of wing at maximum
amplitude of cycle

Solid lines indicate position
of wing at rest

Fraction of semispan

1.0
.9
.8
.7
.6
.5
.4
.3
.2
.1
0

Chord

NACA

Figure 21.- Third natural vibration mode, model B_s.
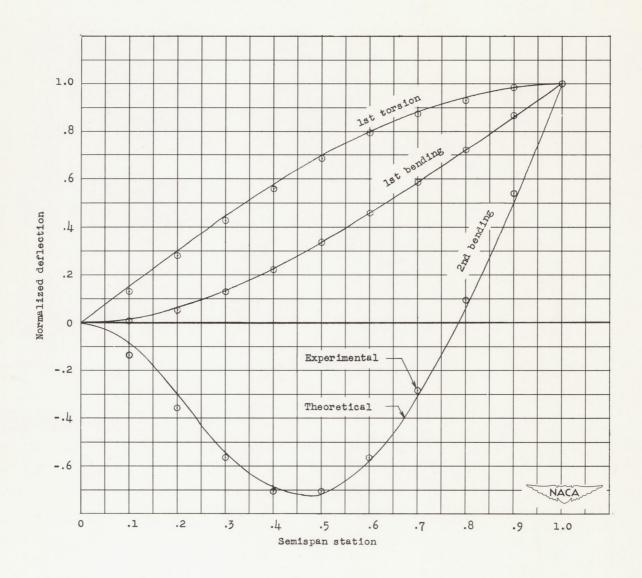
f_3 = 39 cycles per second.

Figure 22.- Comparison of theoretical and experimental vibration modes of an 8- by 50- by 0.25-inch aluminum-alloy plate.